Supplementary information

Macrophage phenotype modulation via 2-hydroxypropyltrimethyl ammonium chloride chitosan: a novel strategy for managing allergic rhinitis

Yi Peng,†[ab] Cuida Meng,†[c] Yu Liu,[ab] Kejia Li,[a] Meng Zhu,[a] Xiaoyan Ju,[a] Ye Tian,[a] Dongdong Zhu,*[c] Zhongwei Niu*[ad]

[a] *Key Laboratory of Photochemical Conversion and Optoelectronic Materials, Technical Institute of Physics and Chemistry, Chinese Academy of Sciences, Beijing 100190, China.*

[b] *University of Chinese Academy of Sciences, Beijing 100049, China.*

[c] *Department of Otorhinolaryngology Head and Neck Surgery, China-Japan Union Hospital of Jilin University, Changchun, China.*

[d] *School of Future Technology, University of Chinese Academy of Sciences, Beijing 100049, China.*

† Yi Peng and Cuida Meng contributed equally to this work.

* Corresponding author. E-mail addresses: zhudd@jlu.edu.cn (D. Zhu), niu@mail.ipc.ac.cn (Z. Niu).

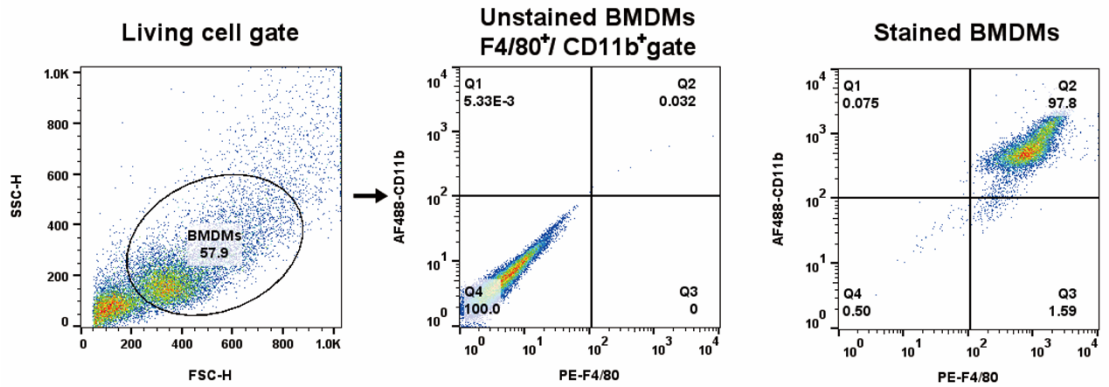

Fig. S1 Gating strategy and purity assessment of BMDMs by flow cytometry. Cell debris was excluded based on FSC-H and SSC-H. The expression of F4/80 and CD11b was analyzed within the live cell population.

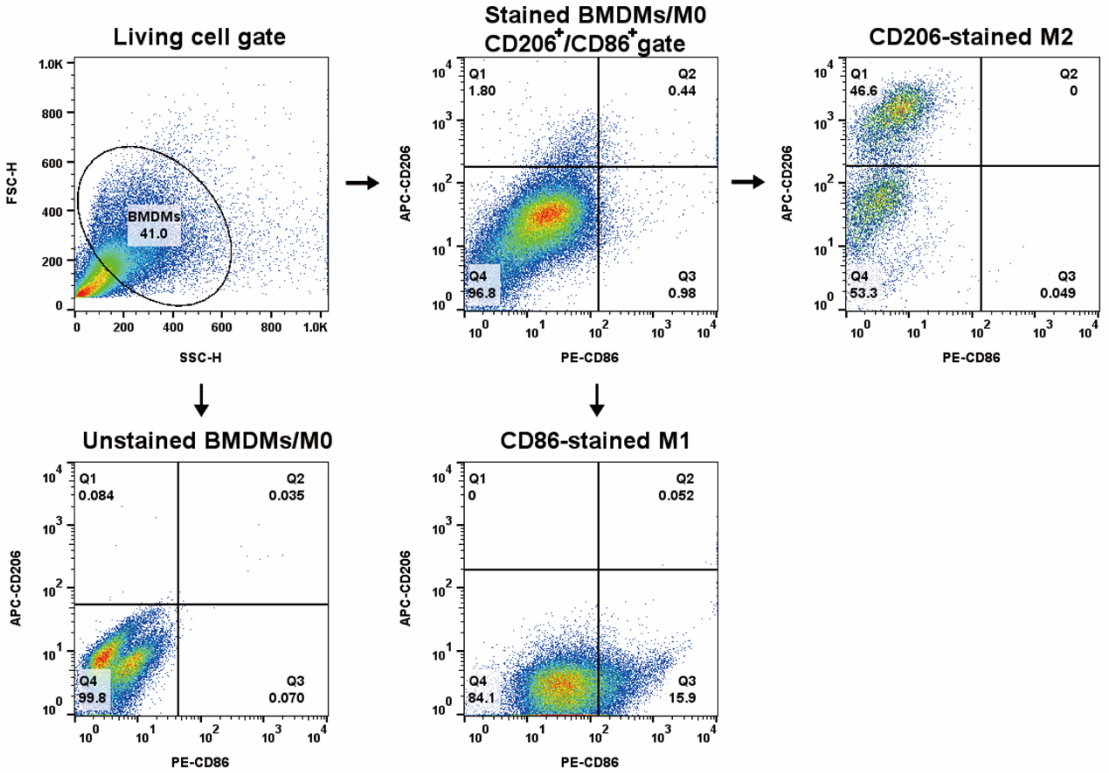

Fig. S2 The gating strategy for detecting CD86 and CD206 expression in BMDMs involved the following steps: First, cell debris was excluded based on FSC-H and SSC-H parameters. Subsequently, the boundaries for $CD86^+$ and $CD206^+$ populations were established according to the expression profiles characteristic of distinct BMDMs phenotypes.

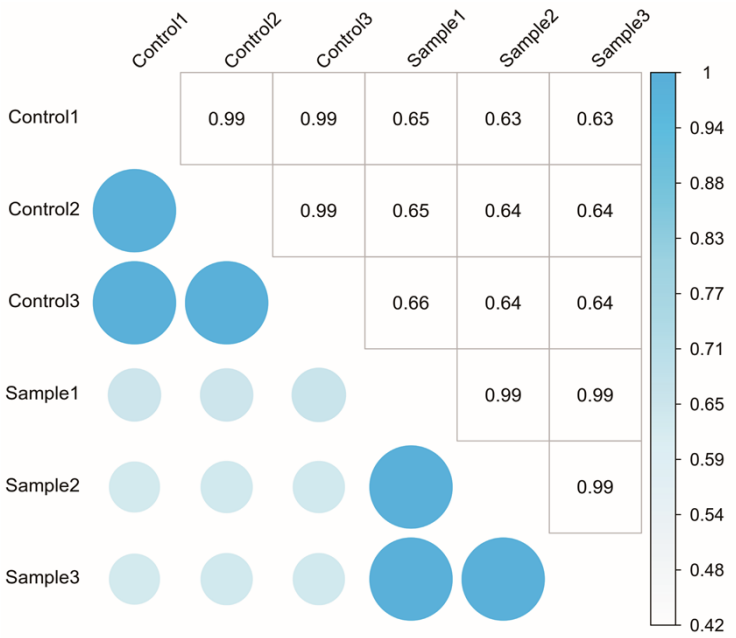

Fig. S3 Inter-Sample Correlation Analysis. The intensity of the blue color corresponds to the magnitude of the correlation coefficient, with darker shades indicating higher similarity between samples (closer to 1). n = 3.

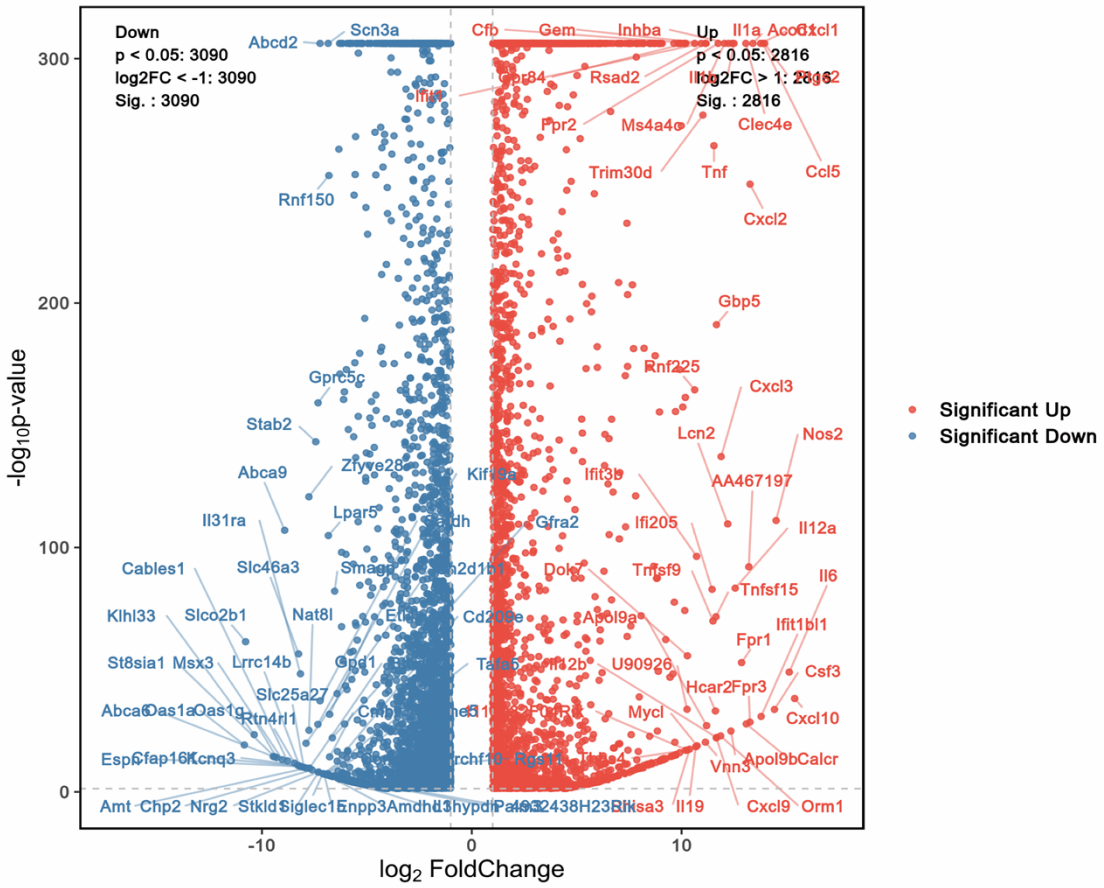

Fig. S4 Volcano plot of differentially expressed genes, displaying the top 50 most significantly up- and down-regulated genes. n=3.

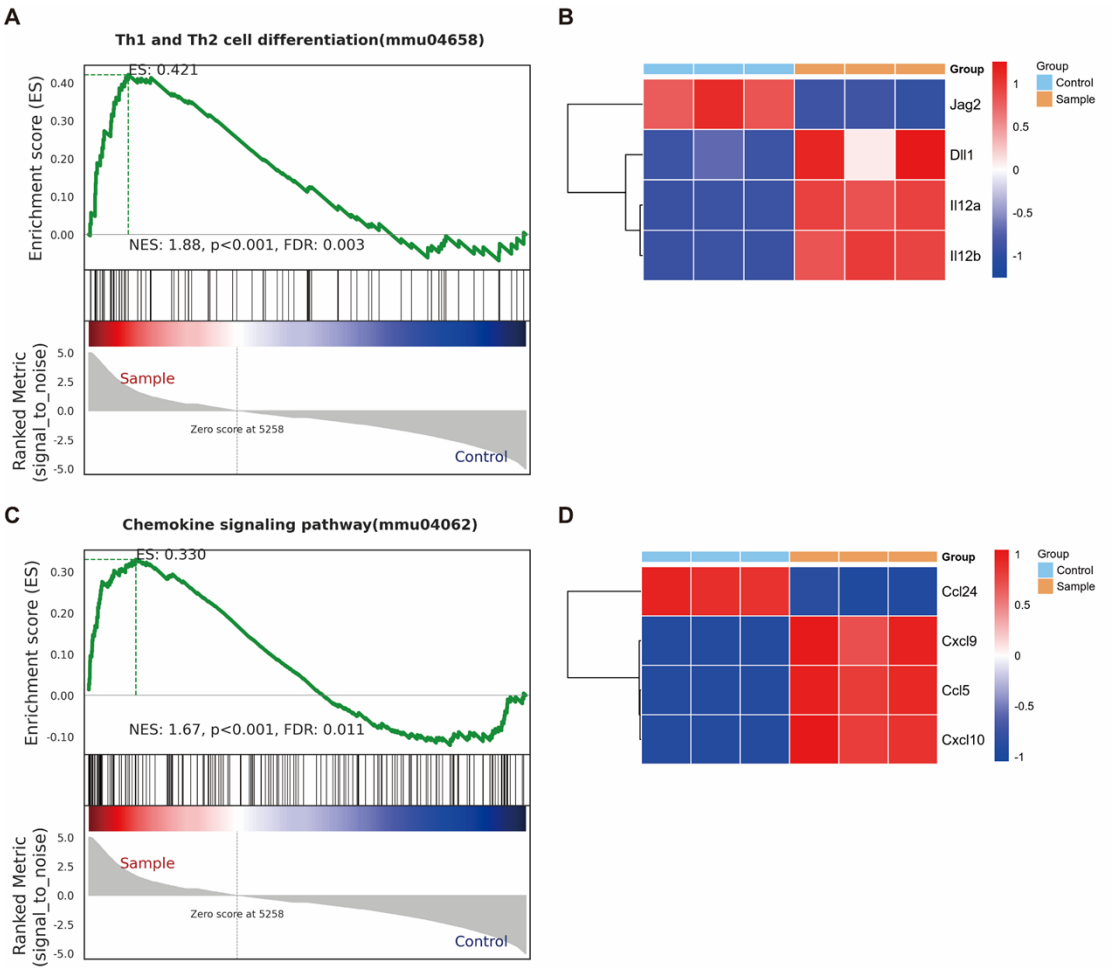

Fig. S5 GSEA enrichment analysis of key pathways and heatmaps of key differentially expressed genes. (A, C) GSEA plots for the Th1 and Th2 cell differentiation (A) and Chemokine signaling pathway (C). (B, D) Heatmap displaying the expression patterns of key differentially expressed genes from the Th1 and Th2 cell differentiation (B) and Chemokine signaling pathway (D). n = 3.

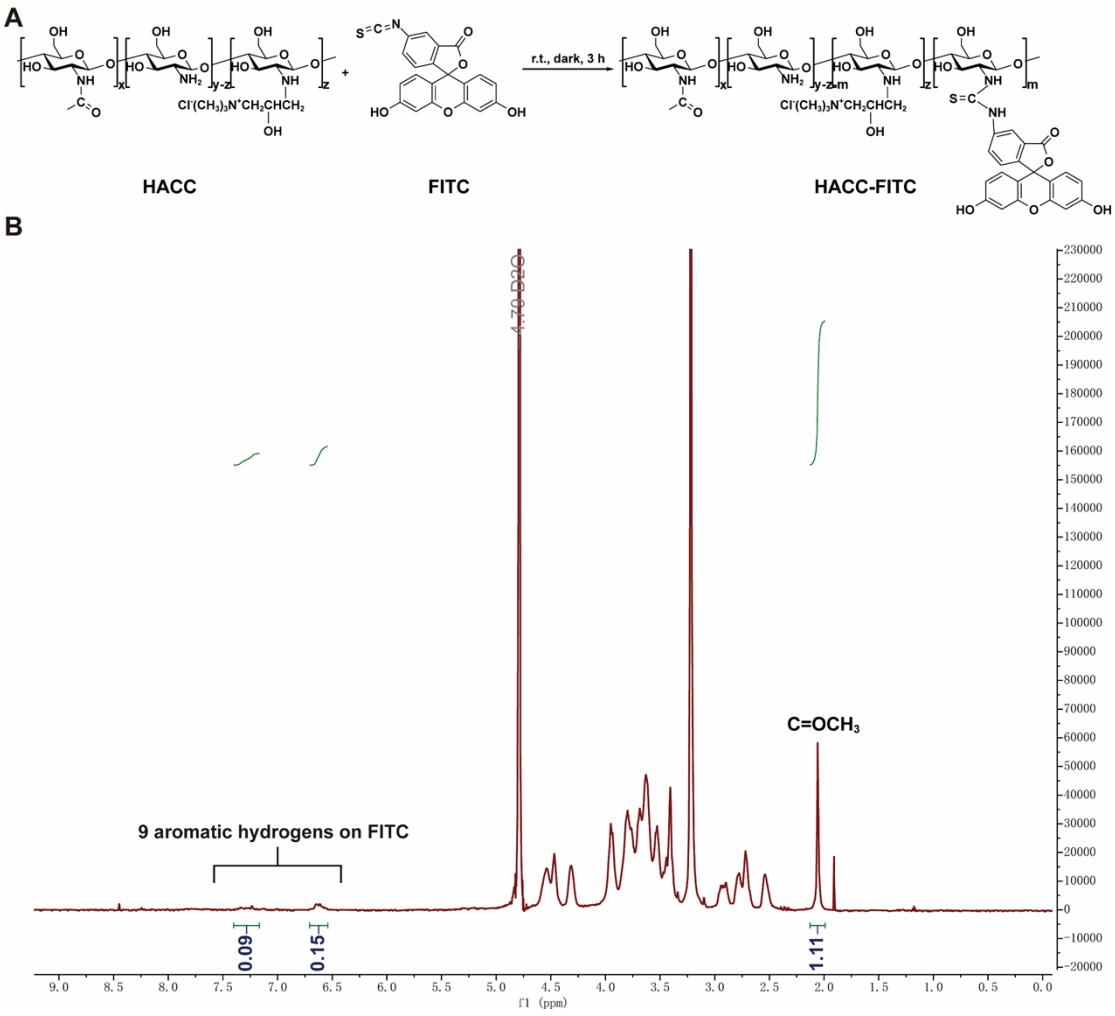

Fig. S6 The (A) preparation and (B) ^{1}H NMR spectrum of HACC-FITC.

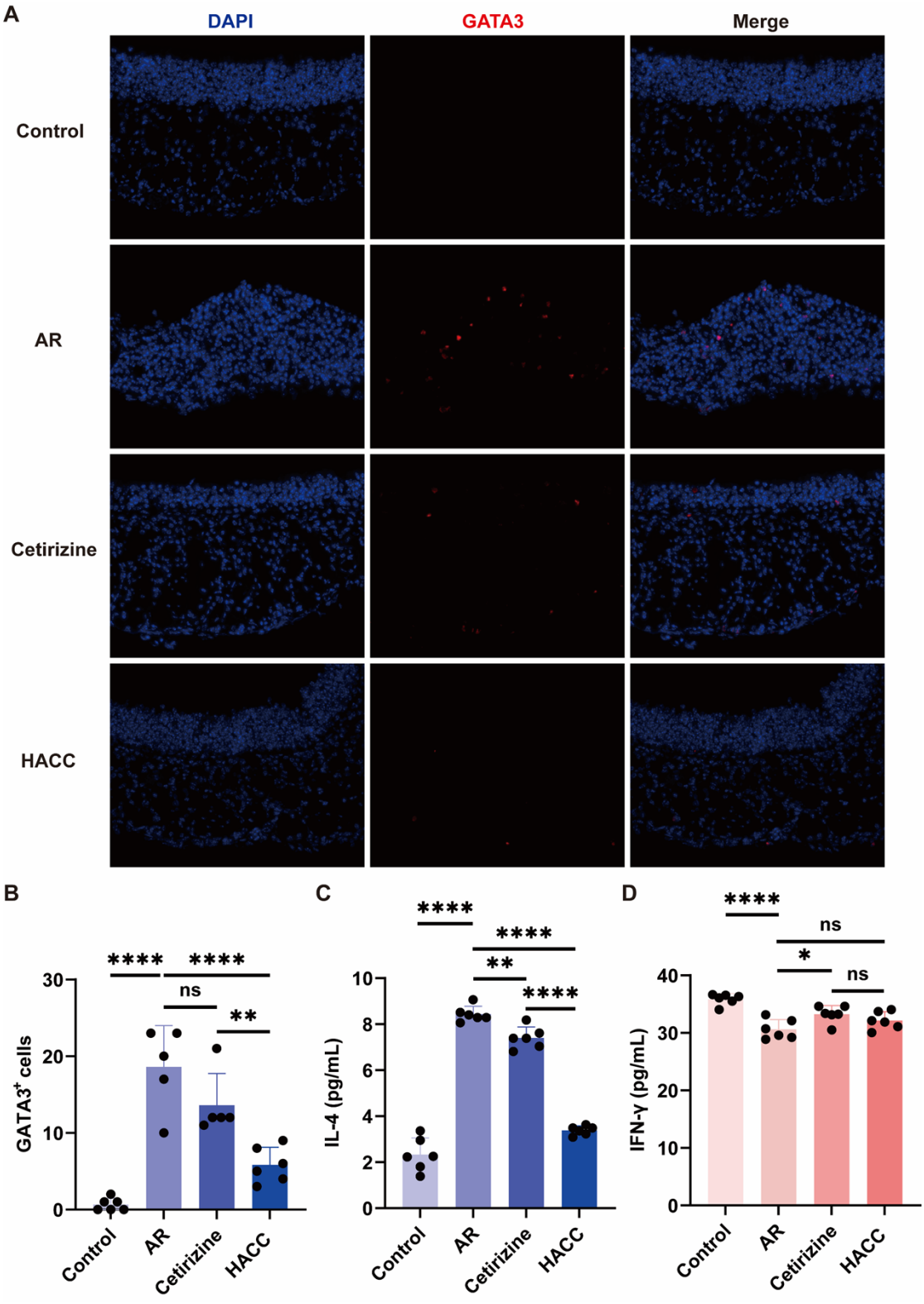

Fig. S7 Expression of GATA3 in nasal mucosa and serum levels of IL-4 and IFN-γ in the AR mouse model. (A) Representative images showing GATA3 expression (red fluorescence) in mouse nasal mucosa at 63 × magnification. Scale bar: 20 μm. (B) Quantitative analysis of GATA3⁺ cells per field under 63 × magnification. n ≥ 5. **p < 0.01; ****p < 0.0001, ns, not significant. (C-D) Serum IL-4 (C) and IFN-γ (D) concentrations in each group of mice. n = 6. *p < 0.05; **p < 0.01; ****p < 0.0001, ns, not significant.

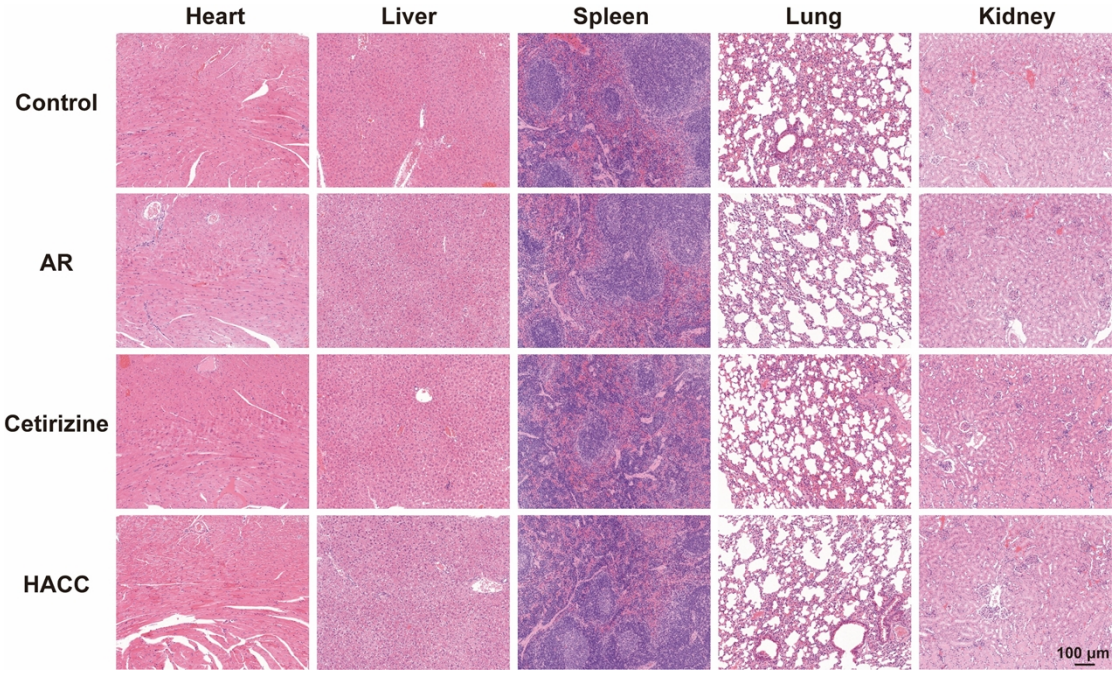

Fig. S8 H&E staining of major organs (heart, liver, spleen, lung, and kidney) in mice. Scale bars: 100 μm.

Table S1 Primer sequences for qRT-PCR.

Gene	Forward Primer	Reverse Primer
β-actin	CACTGTCGAGTCGCGTCC	TCATCCATGGCGAACTGGTG
Cd206	TTCAGCTATTGGACGCGAGG	GAATCTGACACCCAGCGGAA
Arg-1	TAGACAAGCTGGGGATTGGC	ATCGGCCTTTTCTTCCTTCCC
Fizz1	AACTTCTTGCCAATCCAGCTAAC	CCCAGTAGCAGTCATCCCAG
Il10	GCATGGCCCAGAAATCAAGG	ACACCTTGGTCTTGGAGCTTATTA
Ym1	GCTTTTGAGGAAGAATCTGTGG	ACCTGAATATAGTCAAGAGACTGAG
Cd86	CAGCACGGACTTGAACAACC	CTCCACGGAAACAGCATCTGA
Tnfα	CCCTCACACTCAGATCATCTTCT	GCTACGACGTGGGCTACAG
Il1β	TGCCACCTTTTGACAGTGATG	ATGTGCTGCTGCGAGATTTG
Cxcl10	CCACGTGTTGAGATCATTGCC	GAGGCTCTCTGCTGTCCATC